시간 지연을 고려한 로봇 매니퓰레이터의 강인한 임피던스 제어

김재훈, 신현석, 박창우, 박민용
연세대학교 전기컴퓨터공학과 지능제어시스템 연구실
전화 : (02) 361-2868 / 팩스 : (02) 312-2333

Robust Impedance Control of Robot Manipulator Considering Time Delay

Jaehun Kim, Hyunseok Shin, Chang-Woo Park, Mignon Park
Dept. of Electrical and Computer Eng., Yonsei Univ.
E-mail: jackson@yeics.yonsei.ac.kr

Abstract

In this paper we design the robust impedance controller of the robot manipulator with time delay. The designed controller considers time delay in the position loop and stabilizes the closed-loop system. The performance of a controller can be easily degraded by external disturbances. To improve the performance when external disturbances exist, we use the disturbance observer to handle the disturbances in the velocity loop and provide robustness to the control system. To show the validity of the designed controller, several experiments are performed for the 5-DOF robot manipulator equipped with the wrist force/torque sensor system.

1. Introduction

It is desirable to have robot manipulator behave in a controlled compliant manner when performing tasks which require contact with the environment. The two main approaches to the force control problem may be broadly classified as hybrid position/force control, and impedance control. Hybrid position/force control[1] splits the task space into two orthogonal subspaces. Position is controlled along those directions in which it is impossible to apply an arbitrary force. Force is controlled along those directions in which arbitrary motion is not possible. Impedance control[2] is a generalized force/position control approach to unconstrained motion control and constrained manipulation. The objective of impedance control is to regulate the mechanical impedance of the robot manipulator that relates both position and force rather than directly controlling force or position. This ensures that a user specified dynamic relationship between the robot manipulator end-point position, and the robot manipulator environmental contact force can be achieved.

Since the impedance controller of a robot manipulator is often implemented by a digital computer, the sampling frequency affects the stability characteristics of a robot manipulator. In general, a robot manipulator gets the sensory information such as force signal through RS-232C serial communication channel and it takes about 20msec for most of force sensor system to send the measured force with 19200 bps(bit per second). Thus, in case of the robot manipulator with this force sensor system, a sampling frequency cannot be arbitrarily made high. It is noticed that the digital system with time delay can go unstable in the low sampling frequency[3, 4].

External disturbances usually exist in real control situations and can degrade the performance of a controller. Recently, the disturbance observer has been applied to many systems in order to realize fast and accurate control[5, 6].

In this paper, we design the impedance controller stabilizing the robot manipulator with time delay. Also, in order to provide robustness to the control system we use the disturbance observer.

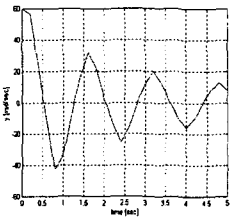

Fig. 2-1 Controller with time delay

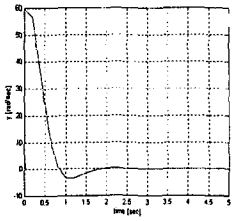

Fig. 2-2 Designed controller

2. Controller with Unit Time Delay

To investigate the problem caused by time delay, consider a discrete-time system.

$$\begin{aligned} \mathbf{x}(k+1) &= \mathbf{A}\mathbf{x}(k) + \mathbf{B}\mathbf{u}(k) \\ \mathbf{y}(k) &= \mathbf{x}(k) \end{aligned} \tag{2-1}$$

If time delay is τ in a controller, the controller becomes

$$\mathbf{u}(kT+\tau) = \mathbf{F}\mathbf{x}(kT) \tag{2-2}$$

Fig. 2-1 shows that the system has oscillation when time delay is a half of the sampling time. We used $\mathbf{A} = e^{-aT}$, $\mathbf{B} = 1 - e^{-aT}$, $a = 0.3, T = 0.2$ in the simulation. In this paper, we design the discrete-time controller to consider time delay in the control loop.

$$\mathbf{u}(k+1) = \mathbf{D}\mathbf{u}(k) + \mathbf{E}\mathbf{x}(k) \tag{2-3}$$

The ideal controller has time delay in real implementation. Since the output of the controller with time delay is not synchronized with the sampling time, it is difficult to design and analyze the controller.

On the contrary, since the output of the designed controller is synchronized with the next sampling time, it is relatively easy to design and analyze the controller. The closed-loop system is

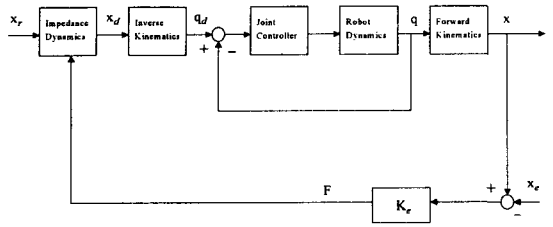

Fig. 3-1 Impedance control

$$\begin{bmatrix}\mathbf{x}(k+1)\\ \mathbf{u}(k+1)\end{bmatrix}=\begin{bmatrix}\mathbf{A} & \mathbf{B}\\ \mathbf{E} & \mathbf{D}\end{bmatrix}\begin{bmatrix}\mathbf{x}(k)\\ \mathbf{u}(k)\end{bmatrix} \tag{2-4}$$

If we define a new state as $\mathbf{w}(k)=[\mathbf{x}(k)\quad \mathbf{u}(k)]^T$, then

$$\mathbf{w}(k+1)=\bar{\mathbf{A}}\mathbf{w}(k)+\bar{\mathbf{B}}\mathbf{v}(k) \tag{2-5}$$

$$\mathbf{v}(k)=-\bar{\mathbf{F}}\mathbf{w}(k) \tag{2-6}$$

where $\bar{\mathbf{A}}=\begin{bmatrix}\mathbf{A} & \mathbf{B}\\ \mathbf{0} & \mathbf{0}\end{bmatrix}, \bar{\mathbf{B}}=\begin{bmatrix}\mathbf{0}\\ \mathbf{I}\end{bmatrix}, \bar{\mathbf{F}}=-[\mathbf{E}\quad \mathbf{D}]$. Therefore we can determine the gains of the designed controller from Eq. (2-5) and (2-6). Fig. 2-2 shows that the designed controller stabilizes the system without oscillation.

3. Discrete-Time Impedance Control

The desired dynamic relation between the actual position of the robot manipulator $\mathbf{x}\in\mathbf{R}^m$, the pre-assigned reference position $\mathbf{x}_r\in\mathbf{R}^m$, and the contact force exerted by the robot manipulator on the environment $\mathbf{F}\in\mathbf{R}^m$ can be defined as

$$\mathbf{M}\ddot{\tilde{\mathbf{x}}}+\mathbf{B}\dot{\tilde{\mathbf{x}}}+\mathbf{K}\tilde{\mathbf{x}}=\mathbf{F} \tag{3-1}$$

where $\tilde{\mathbf{x}}=\mathbf{x}_r-\mathbf{x}; \mathbf{M}\in\mathbf{R}^{m\times m}, \mathbf{B}\in\mathbf{R}^{m\times m}, \mathbf{K}\in\mathbf{R}^{m\times m}$ are inertia, damping and stiffness matrixes respectively. After defining the dynamics relation between the robot manipulator and the environment the objective is to generate the desired dynamics trajectory, $\mathbf{x}_d$, that satisfies the dynamics Eq. (3-1). The solution to this problem is obtained by solving the differential equation

$$\begin{aligned}&\mathbf{M}\ddot{\mathbf{x}}_d(t)+\mathbf{B}\dot{\mathbf{x}}_d(t)+\mathbf{K}\mathbf{x}_d(t)=\\ &-\mathbf{F}(t)+\mathbf{M}\ddot{\mathbf{x}}_r(t)+\mathbf{B}\dot{\mathbf{x}}_r(t)+\mathbf{K}\mathbf{x}_r(t)\end{aligned} \tag{3-2}$$

where $\mathbf{x}_d(0)=\mathbf{x}_r(0), \dot{\mathbf{x}}_d(0)=\dot{\mathbf{x}}_r(0)$. Clearly, in the absence of contact force $\mathbf{F}$,

$$\mathbf{x}_d(t)=\mathbf{x}_r(t),\quad \forall t \tag{3-3}$$

the robot manipulator simply tracks the pre-assigned trajectory $\mathbf{x}_r$; otherwise, it tracks the generated desired dynamics trajectory $\mathbf{x}_d$.

In order to design the discrete-time impedance controller, a discrete-time representation of Eq. (3-1) is required. Assuming the sampling time is T_s, a discrete-time equivalence of Eq. (3-1) is the difference equation

$$\bar{\mathbf{M}}\tilde{\mathbf{x}}(k-2)+\bar{\mathbf{B}}\tilde{\mathbf{x}}(k-1)+\bar{\mathbf{K}}\tilde{\mathbf{x}}(k)=\mathbf{F}(k) \tag{3-4}$$

where $\bar{\mathbf{M}}=\dfrac{\mathbf{M}}{T_s^2}, \bar{\mathbf{B}}=-\dfrac{2\mathbf{M}+T_s\mathbf{B}}{T_s^2}, \bar{\mathbf{K}}=\dfrac{\mathbf{M}+T_s\mathbf{B}+T_s^2\mathbf{K}}{T_s^2}$.

The computation of the discrete-time solution to Eq. (3-2) is straightforward

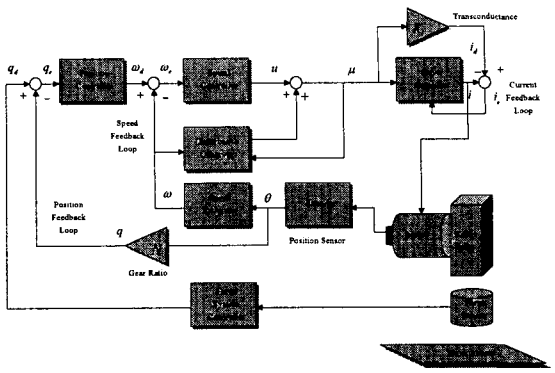

Fig. 4-1 Impedance control using SLC method

$$\begin{aligned}\mathbf{x}_d(k)=&-\bar{\mathbf{K}}^{-1}\mathbf{F}(k)+\bar{\mathbf{K}}^{-1}\bar{\mathbf{M}}\{\mathbf{x}_r(k-2)-\mathbf{x}_d(k-2)\}\\ &+\bar{\mathbf{K}}^{-1}\bar{\mathbf{B}}\{\mathbf{x}_r(k-1)-\mathbf{x}_d(k-1)\}+\mathbf{x}_r(k)\end{aligned} \tag{3-5}$$

The Impedance control system configuration is sown in Fig. 3-1.

4. Design of Impedance Controller

In this paper, we use the 5-DOF robot manipulator that each joint of the robot manipulator is driven by DC servo motor.

4.1 Controller in Velocity Loop

In general, several sensors are used in a robot manipulator, so we choose the multi-rate digital control techniques. Also, since the successive loop closures (SLC) method, one of the multi-rate sampling techniques, is often used in position control of servo motor, we use it in this paper. Fig. 4-1 shows the impedance controller using SLC method.

4.1.1 PI Controller

The function of PI controller is to compute u, which is the input in the current feedback loop, from the velocity input ω_d, which is also the output in the position feedback loop. The pulse transfer function is represented by

$$\frac{U(z)}{\Omega_e(z)}=K^P+\frac{K^I}{1-z^{-1}} \tag{4-1}$$

where K^P is P-gain and K^I is I-gain.

4.1.2 Disturbance Observer (DOB)

In this paper, we use the disturbance observer in the velocity control loop. The disturbance observer was proposed to estimate and cancel out the external disturbances using the high gain characteristics of the robust controller. The estimated disturbance is immediately supplied to the servo system, so that the servo system is not affected by the disturbance. Its basic concept is shown in Fig. 4-2.

To understand how the disturbance observer works, first let $Q(s)=1$ in Fig. 4-2. Then it can be easily verified that

$$\hat{\delta}=\hat{d}=\left(1-\frac{P_n^v}{P^v}\right)u+\frac{1}{P^v}\xi_v+d \tag{4-2}$$

where P^v is the actual plant transfer function for the velocity output, P_n^v is the nominal transfer function, d

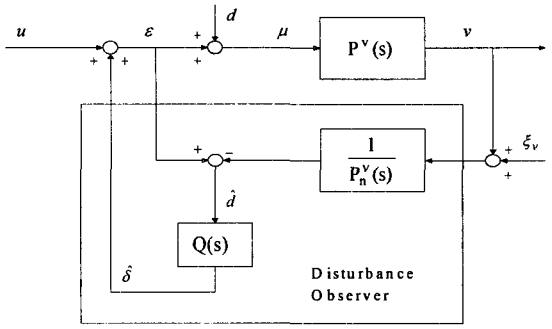

Fig. 4-2 Disturbance observer

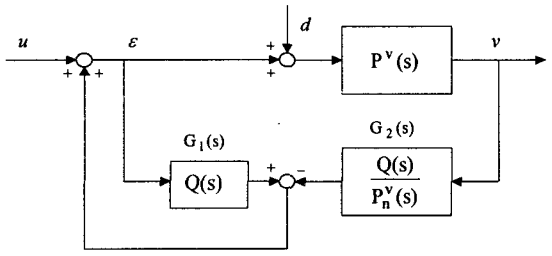

Fig. 4-3 Disturbance observer structure for digital implementation

is the external disturbance, $\hat{d}$ represents the estimate of d, u is the external input to the velocity loop and ξ_v is the measurement noise. The velocity output is then expressed as

$$v = P^v(u - \hat{d} + d) = P_n^v u - \xi_v \qquad (4\text{-}3)$$

Notice that the input-output relation between u and v is characterized by the nominal model.

The disturbance observer cannot be implemented if $Q(s) = 1$. Notice that $1/P_n^v(s)$ is not realizable by itself but that $Q(s)/P_n^v(s)$ can be made realizable by letting the relative degree of $Q(s)$ be equal to or greater than that of $P_n^v(s)$. Furthermore, $Q(s)$ may attenuate the effect of measurement noise appearing in (4-2) and (4-3).

From the block diagram in Fig. 4-2, v is expressed as

$$v = G_{uv}(s)u + G_{dv}(s)d + G_{\xi_v v}(s)\xi_v \qquad (4\text{-}4)$$

where

$$G_{uv} = \frac{P^v P_n^v}{P_n^v + (P^v - P_n^v)Q} \qquad (4\text{-}5)$$

$$G_{dv} = \frac{P^v P_n^v (1-Q)}{P_n^v + (P^v - P_n^v)Q} \qquad (4\text{-}6)$$

$$G_{\xi_v v} = -\frac{P^v Q}{P_n^v + (P^v - P_n^v)Q} \qquad (4\text{-}7)$$

If $Q(s) \approx 1$, the three transfer functions in Eq. (4-4) are $G_{uv} \approx P_n^v, G_{dv} \approx 0, G_{\xi_v v} \approx -1$ and the relation in Eq. (4-2) approximately holds. This implies that the disturbance observer makes the actual plant behave like a nominal plant, and this provides robustness to the control system.

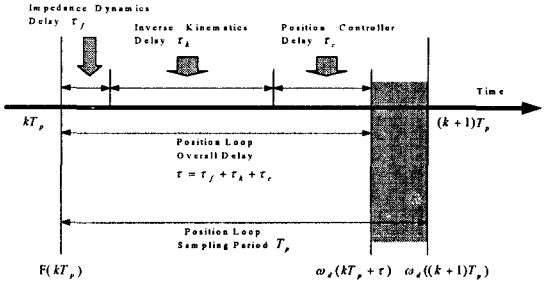

Fig. 4-4 Timing diagram in the position loop

On the other hand, if $Q(s) \approx 0$, the three transfer functions are $G_{uv} \approx P^v, G_{dv} \approx P^v, G_{\xi_v v} \approx 0$ and the open loop dynamics is observed. Therefore, a sensible choice is to let the low frequency dynamics of $Q(s)$ close to 1 for disturbance rejection and model uncertainties. The high frequency dynamics must be close to 0 anyway because the relative degree of $Q(s)$ must be equal or greater than that of $P_n^v(s)$. Sensor noise rejection may be another consideration in selection of $Q(s)$.

A third order binomial filter which satisfies above stated properties has been chosen in this paper

$$Q(s) = \frac{3(\varpi)+1}{(\varpi)^3 + 3(\varpi)^2 + 3(\varpi) + 1} \qquad (4\text{-}8)$$

The disturbance observer can be implemented digitally in several ways. Experimental results in Section 5 were obtained by transforming it into the structure shown in Fig. 4-3 and by applying bilinear transformation to $G_1(s)$ and $G_2(s)$ to convert them into digital filters.

4.2 Controller in Position Loop

4.2.1 Time Delay in Position Loop

The function of the position control loop is to compute ω_d, which is the input in the velocity feedback loop, from the position input q_d, which is derived through force sensor and impedance dynamics. We design the position controller to consider time delay in the control loop. Fig. 4-4 shows the timing diagram in the position loop.

From the figure, if the sampling time is T_p, it takes τ to send the output of the controller to robot manipulator. It is complex to design and analyze the closed-loop system because time delay of the system (τ) is not unit time delay (T_p). On the contrary, since the output of the designed controller in this paper is synchronized with the next sampling time, $(k+1)T_p$, it is relatively easy to design and analyze the controller.

4.2.2 PD Controller

The pulse transfer function of PD controller is represented by

$$\Omega_d(z) = \frac{(K^P + K^D)z - K^D}{z^2} Q_e(z) \qquad (4\text{-}9)$$

where K^P is P-gain and K^D is D-gain. The software

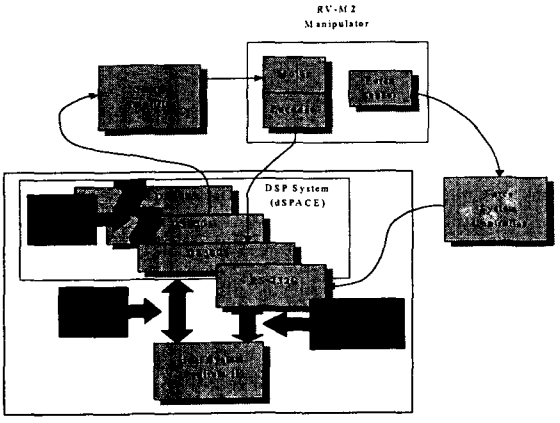

Fig. 5-1 System configuration for experiment

implementation of Eq. (4-9) is

$$\omega_d(k+1) = K^P q_e(k) + K^D\{q_e(k) - q_e(k-1)\} \quad (4\text{-}10)$$

It is noticed that Eq. (4-9) and (4-10) contain the unit time delay.

5. Experiments

In this section, we show the performance of the designed controller by two kinds of experiments: unconstrained motion control and constrained motion control. The impedance parameters for control of the end-effector are given by

$$\mathbf{M} = 125[\mathrm{N/ms^{-2}}], \mathbf{B} = 11180[\mathrm{N/ms^{-1}}], \mathbf{K} = 2500[\mathrm{N/m}]$$

Fig. 5-1 shows the system configuration for experiments.

Case I : Unconstrained motion control

The primary task is to track a line segment in Cartesian space from (x, y) = (0.0, 400.0) [mm] to (x, y) = (120.0, 500.0) [mm]. Fig. 5-2 and 5-3 show the experimental results that are Cartesian position error of the control scheme without DOB and that with DOB. As shown in these figures, we can observe that the robot manipulator shows superior performance at steady-state when DOB is employed.

Case II : Constrained motion control

The end-effector of the robot manipulator is commanded to track a line segment from z = 162.0 [mm] to z = 62.0 [mm] during 5 seconds and to maintain the final position. Fig. 5-4 and 5-5 show the experimental results. We also compare the control scheme with DOB to that with DOB. The contact force is shown in Fig. 5-4 and the position error is shown in Fig. 5-5. In this experiment, we know that when the disturbance observer is used, the desired impedance relation can be achieved more accurately. As shown in Fig. 5-5, the position error to z-axis increases rapidly due to the contact with environment after 5 second.

6. Conclusion

The discrete-time controller which considers time delay in the control loop and stabilizes the closed-loop system was designed. Also, the designed controller was applied to impedance control of a robot manipulator. To reduce the disturbance effects on the system performance, the disturbance observer was used to improve the performance of the system. The performance of the controller using the disturbance observer has been examined through experiments.

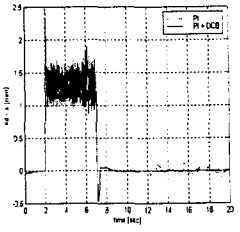

Fig. 5-2 Position error(x-axis)

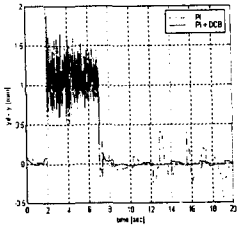

Fig. 5-3 Position error(y-axis)

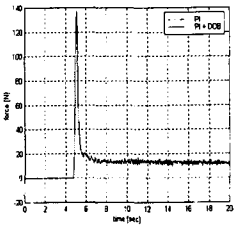

Fig. 5-4 Contact force

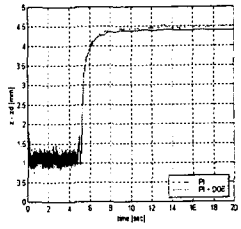

Fig. 5-5 Position error (z-axis)

References

[1] M. H. Raibert and J. J. Craig, "Hybrid position/force control of manipulators," ASME Journal of Dynamic Systems, Measurement and Control, vol. 102, pp.126-133, 1981.

[2] N. Hogan, "Impedance control : an approach to manipulation, Part 1 - Part 3," ASME Journal of Dynamic Systems, Measurement and Control, vol. 107, pp. 1-24, 1985.

[3] D. A. Lawrence, "Impedance control stability properties in common implementations," Proceedings-IEEE Conference on Robotics and Automation, pp. 1185-1190, 1988.

[4] I. H. Suh, K. S. Eom, H. J. Yeo, B. H. Kang, S.-R. Oh, and B. H. Lee, "Explicit fuzzy force control of industrial manipulators with position servo drives," Proceedings of the IEEE/RSJ/GI International Conference on Intelligent Robots and Systems, pp. 657-664, 1994.

[5] M. Nakano, K. Ohnishi, and K. Miyachi, "A robust decentralized joint control based on interference estimation," Proc. of IEEE Int. Conf. on Robotics and Automation, pp. 326-331, 1987.

[6] T. Umeno, and Y. Hori, "Robust speed control of DC servomotors using modern two degree's-of-freedom controller design," IEEE Trans. Ind. Electron., vol. 38, pp. 363-368, 1991.

[7] M. C. Berg, N. Amit, and D. Powell, "Multirate digital control system design," IEEE Trans. Automat. Contr., vol.33, pp. 1139-1150, 1988.

[8] Heinrichs B., Sepehri N., and Thorntontrump A. B., "Position-based impedance control of an industrial hydraulic manipulator," IEEE Control Systems Magazine, vol. 17, pp. 46-52, 1997.